Journal of Catalysis **211,** 379–386 (2002)
doi:10.1006/jcat.2002.3757

Importance of Product Readsorption during Isotopic Transient Analysis of Ammonia Synthesis on Ba-Promoted Ru/Ba*X* Catalyst

Brian C. McClaine and Robert J. Davis[1]

Department of Chemical Engineering, University of Virginia, Charlottesville, Virginia 22904-4741

Received March 7, 2002; revised July 19, 2002; accepted July 25, 2002

Steady-state isotopic transient kinetic analysis was used to evaluate the intrinsic turnover frequency (TOF_{intr}) and the fractional surface coverage of nitrogen-containing species (θ_{NH_x}) on a Ba-promoted Ru/Ba*X* zeolite (~2 wt% Ru) catalyst during ammonia synthesis at 3 atm, 673 K, and a stoichiometric ratio of N_2 and H_2. The artifacts due to inter- and intraparticle readsorption of product ammonia on the kinetic parameters were removed by cofeeding ammonia to the system and varying the total flow rate. The values of TOF_{intr} and θ_{NH_x} determined from the intrinsic lifetime of surface intermediates at zero ammonia pressure were 0.067 s^{-1} and 0.064, respectively. The zeolite-supported catalyst was compared to poorly active Ru/SiO_2 and highly active Cs–Ru/MgO catalysts. Although the TOF_{intr} spanned two orders of magnitude, the value of θ_{NH_x} was fairly independent of support and/or promoter.

Key Words: **ruthenium; ammonia, synthesis of; barium, promotion by; SSITKA; isotopic transient analysis.**

INTRODUCTION

Synthesis of ammonia from dinitrogen and dihydrogen is among the most widely studied catalytic reactions, dating back to the beginning of the 20th century. Iron catalysts, high temperature, and high pressure are usually needed to achieve desirable reaction rates and shift thermodynamic limitations to meet commercial needs. It is advantageous to have a better catalyst due to the high energy demand of operation at these extreme processing conditions. Indeed, production of ammonia requires approximately 1% of the world's power production (1). Interest in ruthenium has been renewed due to the fact it has a higher activity than iron. Ruthenium-based catalysts allow for savings in energy and capital costs due to the fact operation can take place at milder reaction conditions.

Carbon-supported ruthenium that is promoted by alkali metal is already in use as a second-generation ammonia synthesis catalyst (2). However, carbon is not considered an ideal support due to the fact that ruthenium catalyzes both the oxidation and the methanation of carbon (3, 4). The high cost and relatively short lifetime of a Ru/carbon catalyst compared to a conventional iron catalyst, therefore, might outweigh the increase in activity (1).

Zeolites are of particular interest as supports since the maximum size of occluded metal particles is limited to the size of the zeolite pores or cages. Also, the basicity of the zeolite is easily modified by ion exchange with Group IA and IIA cations, with the consensus being that the promoter effectiveness for supported ruthenium catalysts increases with basicity. In particular, we have shown Ru/Ba*X* to be an excellent catalyst for ammonia synthesis when promoted with occluded Ba (5, 6). However, the role of Ba as a promoter for ruthenium-catalyzed ammonia synthesis has not been elucidated. Barium oxide is recognized as a solid base and could act as an electronic promoter of Ru, similar to the function of alkali metals. Promotion of supported ruthenium by Ba has also been attributed to a restructuring of the Ru surface that exposes additional active sites (7–9).

Ammonia synthesis catalysts should be studied under working conditions, if possible, since the reaction is structure sensitive and the catalyst surface structure may depend on the reaction environment. The purpose of the current work was to determine surface coverage and lifetime of nitrogen-containing intermediates on a Ba-promoted Ru/Ba*X* catalyst under reaction conditions using steady-state isotopic-transient kinetic analysis (SSITKA). The current method of SSITKA was first introduced to heterogeneous catalysis by Happel (10) and has been employed previously in a number of studies, including several with catalysts for ammonia synthesis (11, 12). We have also used the method to study a highly active ammonia synthesis catalyst composed of Cs-promoted Ru/MgO (13).

The basic principle of SSITKA is the detection of isotopically labeled species versus time in the reactor effluent following a switch (step change) in the isotopic content of one of the reactant species without disturbing the overall steady-state reaction conditions. Since the switch only involves changing the isotopic label of one of the reactants, the reaction remains isothermal and isobaric. Thus, in the absence of isotopic mass effects, steady-state reaction conditions are maintained throughout the switch. The resulting steady-state kinetic information obtained may include

[1] To whom correspondence should be addressed.

0021-9517/02 $35.00

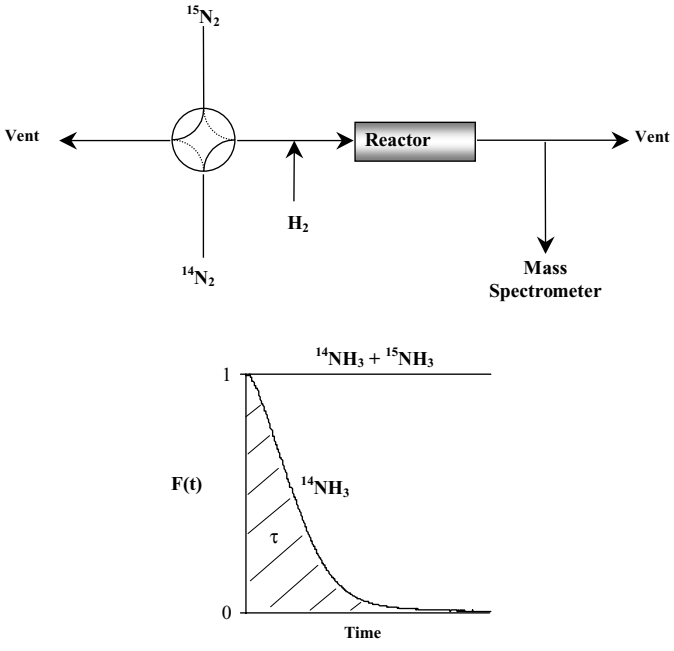

FIG. 1. Experimental setup for steady-state isotopic-transient kinetic analysis (SSITKA) and an example of a typical transient.

surface coverage of different types of adsorbed reaction intermediates, lifetime of surface intermediates, heterogeneity of active sites, and identification of possible reaction mechanisms. A diagram of the reaction system and a typical normalized transient ($F(t)$) can be found in Fig. 1. It should be noted that $F_{^{14}NH_3}(t) = 1 - F_{^{15}NH_3}(t)$, as the sum of the two normalized transients must equal unity in order to maintain the overall steady state. For additional information regarding the SSITKA technique, the reader is referred to the recent review by Shannon and Goodwin (14).

EXPERIMENTAL METHODS

Catalyst Preparation

The catalyst sample was prepared according to the methods described previously (6). Potassium *X* zeolite was obtained by ion exchanging Na*X* zeolite (UOP, Lot 07483-36) three times with a 1 M KNO_3 (Aldrich, 99.9%) aqueous solution for 24 h at room temperature. Incorporation of Ru (~2.0 wt%) was accomplished by ion exchange of the K*X* zeolite in an aqueous solution of $Ru(NH_3)_6Cl_3$ (Alfa Aesar). The Ru^{3+}-exchanged zeolite was then washed with deionized distilled water. The absence of chloride was confirmed by silver nitrate tests of the filtrates. The Ru/K*X* sample was reduced before any further ion exchanges. The sample was first dehydrated by heating under vacuum at 0.5 K min^{-1} to 723 K and maintaining that temperature for 1 h. After cooling to room temperature under vacuum, the dehydrated sample was then heated in flowing H_2 (20 ml min^{-1} g^{-1}, purified by diffusion through Pd, Matheson 8371V) at 1 K min^{-1} to 723 K and reduced at 723 K for an additional 2 h. The Ru/K*X* was finally cooled under vacuum (final pressure, less than 10^{-5} Torr) and placed in a humid atmosphere overnight. The rehydrated Ru/K*X* was ion exchanged three times at room temperature in a 1 M $Ba(CH_3CO_2)_2$ (Aldrich, 99%) solution, filtered, and washed. Barium was added to Ru/Ba*X* beyond ion-exchange capacity by successive impregnations of a 0.15 M solution of $Ba(OH)_2 \cdot 8H_2O$ (Aldrich, 98%) to give a nominal loading of 20 excess Ba atoms per unit cell of zeolite. The catalyst is designated Ba–Ru/Ba*X*.

Cesium-promoted Ru/MgO (~2 wt% Ru) and Ru/SiO_2 (~22 wt% Ru) were also synthesized as reference materials. The samples were prepared by impregnation with $Ru_3(CO)_{12}$ dissolved in THF. The samples then underwent the same reduction procedure described above for the zeolite-supported catalyst. However, several impregnation and reduction steps were required to obtain the desired ruthenium loading for Ru/SiO_2. Cesium was finally added as a promoter in a 1:1 atomic ratio with ruthenium on Ru/MgO by impregnation with aqueous cesium acetate. The acetate was decomposed by heating the catalyst in flowing N_2 (50 ml min^{-1} g^{-1}) at 1 K min^{-1} to 773 K. Additional information regarding the physical characteristics of Cs–Ru/MgO and Ru/SiO_2 can be found in Ref. (13).

Adsorption of Dihydrogen

Dihydrogen chemisorption experiments were performed on a Coulter Omnisorp 100CX instrument. Before chemisorption, a sample was heated in vacuum at 2 K min^{-1} to 673 K, reduced in flowing dihydrogen (99.999% pure and further purified through an OMI-2 purifier) for 30 min at 668 K, and finally outgassed in high vacuum at 673 K for 45 min (final pressure, less than 10^{-6} Torr). The sample was cooled in a vacuum to room temperature for chemisorption. After chemisorption (total), the sample was evacuated at room temperature to remove weakly held hydrogen and a subsequent backsorption (reversible) isotherm was obtained. The amounts of total and reversibly adsorbed hydrogen were calculated by extrapolating the linear part of the adsorption isotherms to zero pressure. The amount of irreversibly adsorbed hydrogen was calculated from the difference between the total and reversible isotherms. To be consistent with earlier work, the hydrogen-based turnover frequencies (TOF_H) were calculated by normalizing the average rate of ammonia production (determined at the reactor outlet) by the number of surface Ru atoms titrated by irreversibly adsorbed hydrogen atoms. However, the fractional surface coverage of nitrogen-containing intermediates (θ_{NH_x}) was based upon the total amount of adsorbed hydrogen.

Isotopic Transient during Ammonia Synthesis

Approximately 260 mg of Ba–Ru/Ba*X* catalyst (sieved between 250 and 425 μm) was loaded into a quartz microreactor (4-mm inside diameter) using quartz wool to hold the sample in place. The sample was heated at 2 K min^{-1} to 723 K in 40 ml min^{-1} of flowing N_2/H_2 (stoichiometric ratio) and held at 723 K for 2 h. The sample was then cooled to the desired temperature to measure reaction rates. Steady-state isotopic transient responses were collected at 673 K while the total flow rate (20, 40, and 60 ml min^{-1}) and the amount of cofed ammonia (0.0, 0.1, and 0.2 ml min^{-1}) were varied in order to examine the effect of ammonia readsorption on the catalyst particles. All switches were performed under stoichiometric conditions and a total pressure of 3 atm.

Normal dinitrogen ($^{14}N_2$) containing a trace amount of argon (1.06%) was supplied by BOC and further purified by passage through a Supelco OMI-2 purifier. Argon was included in order to determine the gas-phase holdup of the reactor system. The concentration of Ar was not sufficient to disturb the steady state during the switches. To ensure the same level of purity, the labeled dinitrogen (98+%, $^{15}N_2$ Isotec) was also purified by passage through a Supelco OMI-2 purifier. Dihydrogen (99.999%, BOC) was purified by diffusion through Pd (Matheson 8371V). Mass flow controllers were used to control the flow rates of these gases. A fused silica capillary (0.05-mm id) approximately 4 m in length was used to introduce ammonia into the system when cofeeding was desired. The flow rate of ammonia was controlled by adjusting the pressure regulator on the ammonia cylinder, thus creating the desired pressure drop across the capillary. The cofed ammonia (anhydrous) was not further purified.

The isotopic transient responses were acquired by switching between different feed streams of isotopically labeled dinitrogen ($^{14}N_2/Ar \rightarrow {}^{15}N_2$). To reduce the amount of gas being switched, dihydrogen and ammonia (when appropriate) were introduced to the system after the switching valve. An electronically operated pneumatic valve was used for switching between normal and labeled streams. A perturbation-free switch was accomplished by use of backpressure regulators, which maintained the reactor and vent lines at the same pressure. The concentrations of $^{14}NH_2$, $^{14}NH_3$, $^{15}NH_3$, $^{14}N_2$, $^{14}N^{15}N$, $^{15}N_2$, and Ar ($m/e = 16, 17, 18, 28, 29, 30$, and 40, respectively) were continuously monitored by a Balzers–Pfeiffer Prism 200 amu mass spectrometer. The mass spectrometer housing and transfer lines were maintained at 443 K to minimize ammonia adsorption. The signal for $^{14}NH_2$ ($m/e = 16$) was monitored due to the level of fragmentation that resulted from an electron excitation energy of 40 eV. The reverse switch was performed ($^{15}N_2 \rightarrow {}^{14}N_2/Ar$) in a similar manner. The mass spectrometer was calibrated for ammonia pressure by monitoring the effluent of the reactor that achieved thermodynamic equilibrium.

No evidence of ammonia formation was found in an empty reactor under typical reaction conditions. However, holdup of ammonia was observed when the empty reactor was subjected to a step change in ammonia concentration, resulting in a characteristic τ_{NH_3} associated with the system.

RESULTS

The ruthenium content and dihydrogen uptake of the catalysts are summarized in Table 1. Results from total hydrogen chemisorption were used to calculate the average particle diameter of the ruthenium clusters, d_p, assuming a stoichiometry of 1 H atom per surface Ru atom. Coordination numbers found from Ru *K* edge EXAFS analysis of analogous zeolites samples (15) correspond to average particle diameters of about 0.8 nm, which agrees fairly well with the result based on total hydrogen chemisorption (Table 1). Chemisorption also identified a high dispersion for Cs–Ru/MgO and Ru/SiO_2.

An Arrhenius-type plot showing the effect of temperature on the turnover frequency evaluated at $H_2/N_2 = 3$ and constant total flow rate (40 ml min^{-1}) for the Ba–Ru/Ba*X* catalyst can be found in Fig 2. The turnover frequencies for Cs-promoted Ru/MgO and Ru/SiO_2 are also shown in Fig. 2, for comparison (13). The turnover frequencies in Fig. 2 were based on the ammonia production rates divided by the number of sites counted by irreversible H_2 chemisorption. The Ru/SiO_2 sample was clearly the least active catalyst. However, the turnover frequency on Ba–Ru/Ba*X* was only about a factor of 2 lower than that on Cs-promoted Ru/MgO.

Figure 3 illustrates the effect of the average ammonia partial pressure on the turnover frequency (TOF_H) for the Ba-promoted Ru/Ba*X* catalyst. The average ammonia partial pressure was determined from

$$P_{NH_3,ave} = \frac{\left(P_{NH_3,feed} + P_{NH_3,outlet}\right)}{2}, \qquad [1]$$

where $P_{NH_3,feed}$ and $P_{NH_3,outlet}$ are the partial pressures of ammonia in the reactor feed and outlet, respectively. The TOF_H decreased with increasing partial pressure of

TABLE 1

Characterization of Supported Ruthenium Catalysts

Catalyst	Ru (wt%)	H/Ru_{tot}	H/Ru_{irr}	d_p[a] (nm)
Ba–Ru/Ba*X*[b]	1.41	1.10	0.59	<1.0
Cs–Ru/MgO[c,d]	1.75	0.95	0.63	1.0
Ru/SiO_2[c]	21.9	0.54	0.37	1.9

[a] Calculated particle diameter based on results from total H_2 chemisorption.

[b] 30.4 wt% Ba.

[c] Results obtained from Ref. 13.

[d] 2.86 wt% Cs.

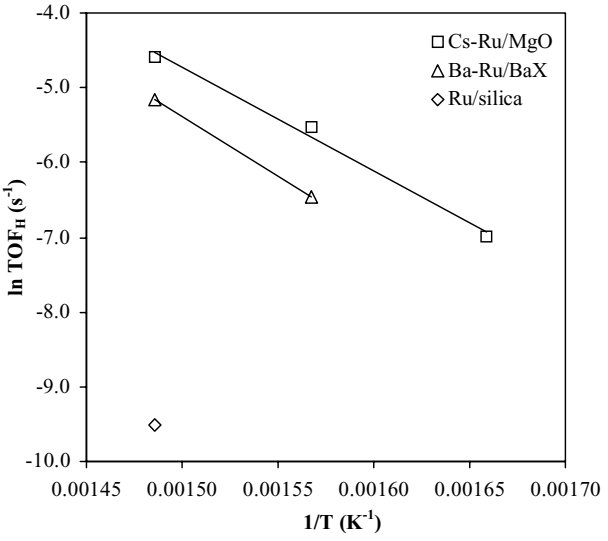

FIG. 2. Arrhenius-type plot for Ba-promoted Ru/BaX (△) catalyst at a $N_2 : H_2$ ratio of 1 : 3, total flow rate of 40 ml min^{-1}, and pressure of 3 atm. The turnover frequency was based on the steady-state ammonia pressure at the reactor outlet and irreversible hydrogen chemisorption (TOF_H). Cs-promoted Ru/MgO (□) and Ru/SiO_2 (◇) are shown for reference.

ammonia in the reactor, resulting in a reaction order of approximately −0.5. It is interesting that results at 20 atm for a similar Ba–Ru/BaX catalyst resulted in an ammonia reaction order of nearly zero (5, 6). The greater apparent inhibition of Ba-promoted Ru by ammonia at 3 atm compared to that at 20 atm might result from operation of the catalyst closer to equilibrium conversion at lower pressure.

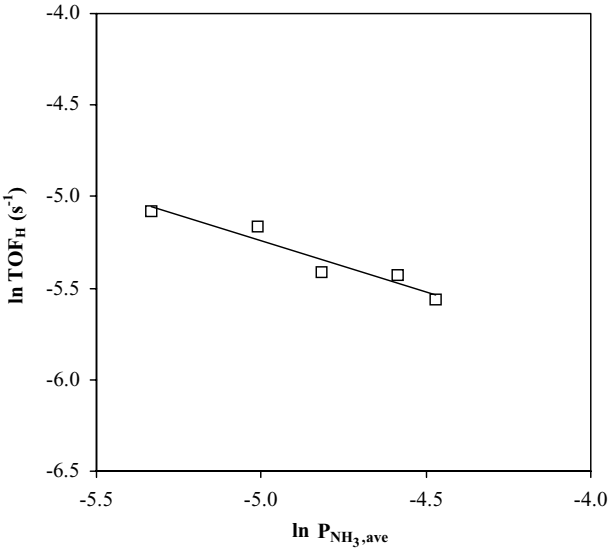

FIG. 3. Effect of flow rate on TOF_H for Ba–Ru/BaX at 673 K and 3 atm with varying levels of cofed ammonia to the reactor. The average mole fraction of ammonia, $P_{NH_3,ave}$, was determined by $P_{NH_3,ave} = (P_{NH_3,feed} + P_{NH_3,outlet})/2$.

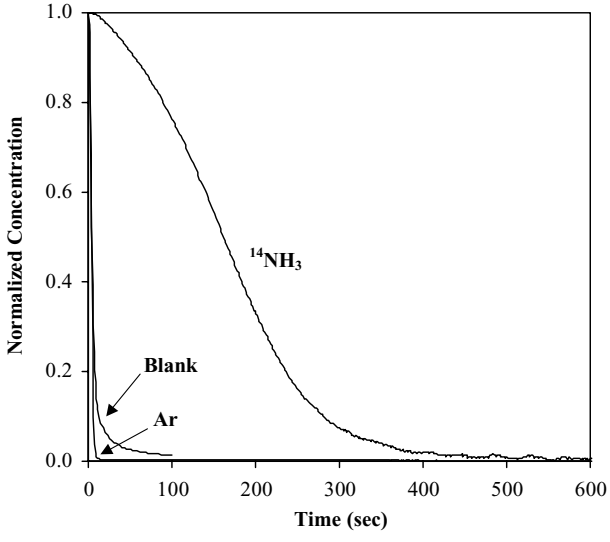

FIG. 4. Typical isotopic transients of $^{14}NH_3$ and Ar at $N_2 : H_2 = 1 : 3$, 40 ml min^{-1}, 673 K, and 3 atm for Ba–Ru/BaX. The transient for ammonia in a blank reactor is also shown.

Steady-State Isotopic Transient Analysis

A typical set of normalized isotopic transients for $^{14}NH_3$ and Ar obtained for the Ba–Ru/BaX catalyst at 673 K and 40 ml min^{-1} following a switch from $^{14}N_2$/Ar to $^{15}N_2$ can be found in Fig. 4. The holdup of ammonia in the system is also shown by the ammonia transient curve in a blank reactor. The average residence time of surface intermediates leading to ammonia (τ_{NH_3}) was calculated by integrating the area between the normalized transients; i.e.,

$$\tau_{NH_3} = \int_0^\infty \left[F_{^{14}NH_3}(t) - F_{^{14}NH_3,blank}(t)\right] dt, \qquad [2]$$

where $F_{^{14}NH_3}$ and $F_{^{14}NH_3,blank}$ are the normalized transient responses for $^{14}NH_3$ and the corresponding blank, respectively.

Ali and Goodwin found that product readsorption had a substantial impact on the determination of surface reaction parameters obtained from transient analysis during methanol synthesis on Pd/SiO_2 (16–18). In light of the fact that ammonia is capable of readsorbing on ruthenium sites active for ammonia synthesis, as well as on inactive ruthenium sites and on the zeolite support itself, the flow rate was varied to alter the residence time of the ammonia in the reactor. The effect of flow rate on the zeolite-based catalyst at 673 K is given in Fig. 5. By extrapolating τ_{NH_3} to infinite flow rate ($1/F = 0$), a better estimate of the surface lifetime due to reaction ($\tau^0_{NH_3}$) can be calculated. This value was found to be 34 s at 673 K. Evidently, readsorption of ammonia results in a large overestimation of τ_{NH_3} and must be correctly accounted for in the analysis. Since increasing the total flow rate eliminates only the effect of interparticle

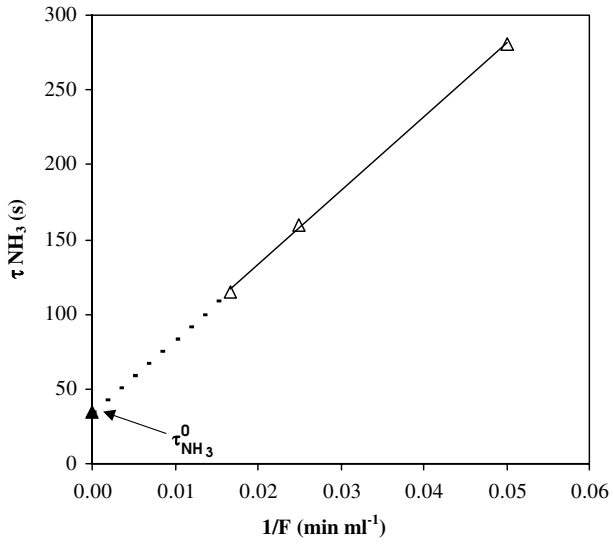

FIG. 5. τ_{NH_3} as a function of flow rate for Ba-promoted Ru/BaX (Δ) catalyst in the absence of any cofed ammonia (used to determine $\tau^0_{NH_3}$).

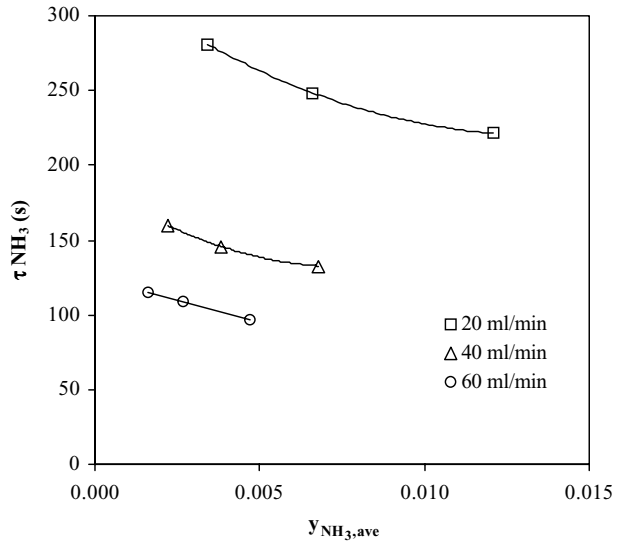

FIG. 6. Effect of $y_{NH_3,ave}$ on τ_{NH_3} for Ba–Ru/BaX at 673 K and 3 atm with $N_2 : H_2 = 1:3$. The average mole fraction of ammonia, $y_{NH_3,ave}$, was determined by Eq. [1].

readsorption, $\tau^0_{NH_3}$ is still an overestimation of the intrinsic surface lifetime due to ammonia readsorption within the zeolite micropores. One way to minimize the intrazeolitic readsorption of product ammonia is to simultaneously cofeed unlabeled ammonia. The cofed ammonia will competitively adsorb in the catalyst pores, thus minimizing the readsorption of ammonia formed by reaction. Variation of the cofed ammonia pressure allows the effect of ammonia readsorption to be decoupled from the observed lifetime of catalytic reaction intermediates.

We have examined the effect of P_{NH_3} on τ_{NH_3} for various flow rates in order to remove artifacts from both inter- and intraparticle ammonia readsorption. This was accomplished by simultaneously feeding unlabeled ammonia ($^{14}NH_3$) into the reactant stream together with $^{14}N_2$ and H_2 and performing an isotopic switch to $^{15}N_2$ while still cofeeding $^{14}NH_3$. The results from these experiments are summarized in Table 2. The relationships between $y_{NH_3,ave}$ and τ_{NH_3} are presented in Fig. 6. Although the total flow rate had a greater impact on τ_{NH_3} than did $y_{NH_3,ave}$, τ_{NH_3} still decreased with increasing $y_{NH_3,ave}$. Clearly cofed ammonia competed for adsorption on all types of sites (i.e., active and inactive).

Values of τ_{NH_3} at constant $y_{NH_3,ave}$ can be derived from data in Fig. 6. Figure 7 presents the dependence of τ_{NH_3} on the flow rate, but now at constant ammonia pressure ($P_{NH_3} = 0.010$ (O), 0.012 (Δ), 0.014 ($\square$) atm). As expected, τ_{NH_3} decreased with the increase of flow rate. By extrapolating the data in Fig. 7 to infinite flow rate ($1/F = 0$), a

TABLE 2

NH_3 SSITKA Results for Ba–Ru/BaX Catalyst at 673 K and 3 atm

Run	Flow rate (ml min^{-1})	$P_{NH_3,feed}$ (atm)	$P_{NH_3,outlet}$ (atm)	TOF_H[a] (10^{-4} s^{-1})	τ_{NH_3} (s)
7	60	0.0000	0.0097	62	115
8	60	0.0046	0.0116	44	109
9	60	0.0119	0.0162	28	97
10	40	0.0000	0.0133	57	160
11	40	0.0070	0.0159	39	146
12	40	0.0179	0.0229	21	133
13	20	0.0000	0.0204	44	281
14	20	0.0139	0.0258	25	248
15	20	0.0358	0.0368	2	222

[a] Based on irreversible H_2 chemisorption.

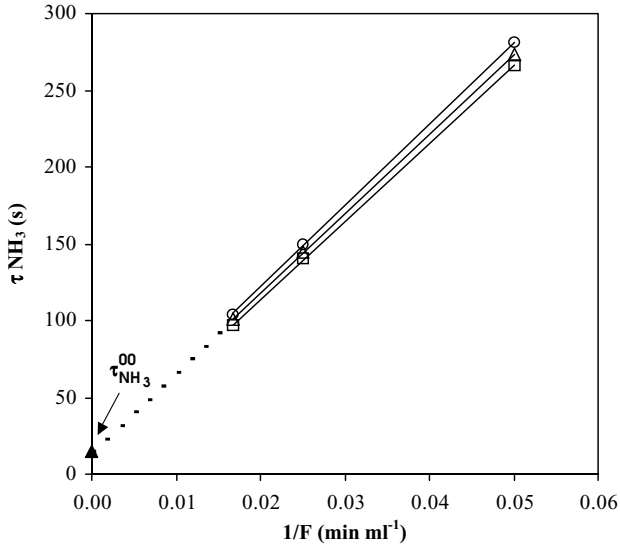

FIG. 7. Effect of flow rate at constant $y_{NH_3,ave}$ during steady-state ammonia production at 673 K and 3 atm with stoichiometric $N_2 : H_2$ for Ba-promoted Ru/BaX with $P_{NH_3,ave} = 0.010$ (○), 0.012 (Δ), 0.014 ($\square$) atm (used to determine $\tau^{00}_{NH_3}$).

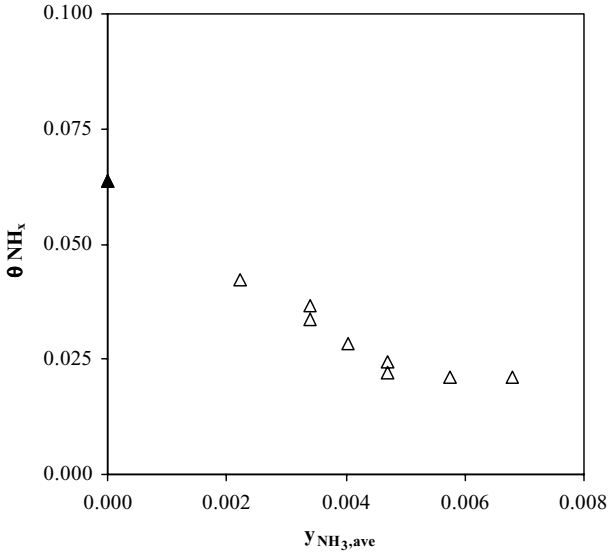

FIG. 8. Effect of $y_{NH_3,ave}$ on the determination of surface coverage of nitrogen-containing intermediates during steady-state ammonia production at 673 K and 3 atm with stoichiometric $N_2:H_2$ for Ba-promoted Ru/Ba*X*. Solid point (▲) is a result of extrapolation of the rate to zero conversion using a Langmuir–Hinshelwood form of the rate equation.

value of τ_{NH_3} that is corrected for both inter- and intraparticle readsorption of ammonia can be obtained ($\tau^{00}_{NH_3}$). The average $\tau^{00}_{NH_3}$ calculated from the runs was found to be 15 ± 2 s, which is about a factor of 2 lower than that found after the removal of interparticle readsorption effects ($\tau^{0}_{NH_3} = 34$ s). Elimination of intraparticle readsorption artifacts was necessary to obtain an intrinsic τ_{NH_3} in a zeolite-supported catalyst.

Figure 8 shows the corresponding fractional coverage of nitrogen-containing intermediates for the Ba-promoted Ru/Ba*X* catalyst. The fractional coverage of nitrogen-containing species was determined from

$$N^{00}_{NH_x} = \tau^{00}_{NH_3} R_{NH_3}, \qquad [3]$$

where R_{NH_3} is the steady-state rate of ammonia formation at the corresponding condition. If the value of $\tau^{0}_{NH_3}$ (determined by removing only effects of interparticle readsorption of ammonia) were used in Eq. [3], then the determination of the number of surface intermediates would have been overestimated. In the absence of intra- and interparticle readsorption artifacts, the fractional surface coverage of N-containing intermediates on Ba-promoted Ru/Ba*X* was found to be less than 10% of surface ruthenium atoms counted by total hydrogen chemisorption for the conditions examined. Extrapolation to $y_{NH_3} = 0$ gives a surface coverage of nitrogen-containing intermediates of 0.064. The solid point in Fig. 8 (▲) was obtained by extrapolating the observed rate to zero ammonia pressure using a Langmuir–Hinshelwood form of the rate equation. The slight decrease in surface coverage with increasing $y_{NH_3,ave}$ is due to an increase in competition for active sites for ammonia synthesis with cofed $^{14}NH_3$.

DISCUSSION

Earlier results from our lab indicated that Ru-loaded zeolites containing occluded Ba were excellent catalysts for ammonia synthesis (5, 6). In fact, Ru/zeolites containing occluded Ba were superior to those containing occluded K (5). Others have also found Ba to be an excellent promoter for ruthenium on a variety of other supports, such as activated carbon and magnesia (7–9, 19–24). However, the mechanism of Ru promotion by basic metals and metal oxides is an open question at this time. The promoter might enhance the rate of ammonia synthesis by lowering the barrier for dinitrogen dissociation (the rate-determining step), by lowering the coverage of nitrogen-containing intermediates (thus freeing sites) or by restructuring the Ru surface to create additional active sites (7, 8, 25–29).

After the effects of inter- and intraparticle readsorption were removed, the value of $\tau^{00}_{NH_3}$ is a good approximation of the intrinsic activity of the active sites, as determined by

$$TOF_{intr} = 1/\tau^{00}_{NH_3}. \qquad [4]$$

The intrinsic turnover frequency (TOF_{intr}) over Ba–Ru/Ba*X* at 673 K was found to be 0.067 s^{-1}. Table 3 compares the results from SSITKA of zeolite-supported Ru to unpromoted Ru/SiO_2 and Cs-promoted Ru/MgO. The nonzeolitic catalysts were not significantly affected by product readsorption (13). The intrinsic turnover frequency on Ba–Ru/Ba*X* was a factor of 40 times greater than that found on unpromoted Ru/SiO_2. However, the zeolite-supported Ru catalyst was about a factor of 2 less active than Cs-promoted Ru/MgO at the same temperature and pressure (13).

All three catalysts revealed a surface coverage of nitrogen-containing intermediates of less than 10% although the intrinsic rate spanned two orders of magnitude. Therefore, the most important implication of the transient analysis presented in this work is that only a small fraction

TABLE 3

Comparison of NH_3 SSITKA Results at 673 K and 3 atm

Catalyst	TOF_H[a] (10^{-4} s^{-1})	$\tau_{NH_3,intr}$ (s)	θ_{NH_x}[b]	TOF_{intr}[c] (10^{-4} s^{-1})
Ru/SiO_2[d]	0.65	670	0.030	15
Ba–Ru/Ba*X*[e]	79	15	0.064	670
Cs–Ru/MgO[d]	109	7.1	0.051	1410

[a] Based on irreversible H_2 chemisorption.
[b] Based on total H_2 chemisorption.
[c] Calculated from $1/\tau_{NH_3,intr}$.
[d] Results obtained from Ref. (13), at a reactant flow rate of 40 ml min^{-1}.
[e] Extrapolated to $y_{NH_3} = 0$.

of the ruthenium surface appears to be involved with dinitrogen dissociation and ammonia synthesis. Dinitrogen activation on a Ru single crystal was recently found to be totally dominated by the steps in the surface which act as low-barrier channels to populate terraces (30, 31). This so-called B_5 site is believed to be responsible for the activity of ruthenium catalysts. Jacobsen *et al.* have recently estimated the relative number of B_5 sites on ruthenium particles of various sizes using crystal models that expose only (001) and (100) hcp surface planes (32). The fraction of active surface ruthenium atoms covered by adsorbed nitrogen species on Ba–Ru/Ba*X* was about a factor of 2–3 lower than that of the B_5 site density predicted by the single-crystal models of similarly sized Ru particles (32). This difference might be due to the crystal morphology assumed by Jacobsen *et al.* in determining the number of B_5 sites or the crystal size distribution of our catalyst. To address the first issue, it should be noted that Jacobsen *et al*. assumed an ideal surface model, which may over predict the number of B_5 sites on a working catalyst. Datye *et al.* have shown using transmission electron microscopy that the shape of Ru clusters on magnesia and silica depends on their size, with smaller crystallites being spherical and larger crystallites being ellipsoidal in shape (33). As for the cluster size distribution, clusters less than 1 nm in diameter are relatively inactive due to the fact that very few B_5 sites are exposed. Therefore, if a substantial fraction of our zeolite-supported ruthenium particles is less than this critical size, then the ruthenium will not be effectively utilized. Finally, competitive adsorption of hydrogen on active sites might lower the fractional surface coverage of nitrogen intermediates. Ruthenium catalysts are well recognized as being inhibited by H_2 during ammonia synthesis.

Using transmission electron microscopy (TEM), Cisneros and Lunsford found that ruthenium particles were uniformly dispersed throughout zeolite *X*, with particle sizes ranging from 0.7 to 2.5 nm (34). Similar results were found using static dihydrogen chemisorption (1–3 nm). The observation that some Ru particles exceeded the internal diameter of the larger zeolite cavities (1.3 nm) was attributed to crystallites in adjacent supercages joined at the windows (35) or defects in the zeolite structure (34).

The promotional effect of occluded barium in Ba*X* zeolite appears to be due not to the creation of new active ruthenium sites but to an enhancement of the existing active sites on the Ru surface. This explanation is supported by the similar surface coverage found on Ru/SiO_2 (within a factor of 2), a catalyst which is 40 times less active than the Ba-promoted Ru/Ba*X*. Evidently, Ba in zeolite *X* acts as an electronic promoter of Ru, similar to alkali metal compounds, and not as a structural promoter, as suggested by others (7–9). Recently published high-resolution transmission electron micrographs of a Ba-promoted Ru metal catalyst for ammonia synthesis revealed an amorphous Ba phase covering part of the Ru surface without altering the morphology of the Ru crystallite (36). The authors of that study therefore concluded that Ba acts as an electronic promoter, which is consistent with the results of our isotopic transient analysis.

CONCLUSIONS

The intrinsic turnover frequency of ammonia synthesis on Ba–Ru/Ba*X* was found to be 0.067 s^{-1} at 673 K and 3 atm total pressure. The coverage of nitrogen-containing intermediates was determined to be 6.4% of the surface ruthenium atoms. This result suggests that only a small fraction of surface ruthenium atoms was active for ammonia synthesis, which is consistent with results found earlier for Cs–Ru/MgO and Ru/SiO_2 under similar conditions. The relative invariance of surface coverage on catalysts with widely varying activities suggests that basic compounds act as electronic promoters of Ru for ammonia synthesis.

ACKNOWLEDGMENTS

This work was supported by a grant from the National Science Foundation (CTS-9729812). Helpful discussions with Prof. James Goodwin regarding the transient experiments are also acknowledged.

REFERENCES

1. Jacobsen, C. J. H., *Chem. Commun.* 1057 (2000).
2. Chementator, *Chem. Eng.* **3**, 19 (1993).
3. Goethel, P. J., and Yang, R. T., *J. Catal.* **111**, 220 (1988).
4. Baker, R., *Carbon*, **24**, 715 (1986).
5. Becue, T., Davis, R. J., and Garces, J., *J. Catal.* **179**, 129 (1998).
6. McClaine, B. C., Becue, T., Lock, C., and Davis, R. J., *J. Mol. Catal.* **163**, 105 (2000).
7. Szmigiel, D., Bielawa, H., Kurtz, M., Hinrichsen, O., Muhler, M., Rarog, W., Jodzis, S., Kowalczyk, Z., Znak, L., and Zielinski, J., *J. Catal.* **205**, 205 (2002).
8. Rarog, W., Kowalczyk, Z., Sentek, J., Skladanowski, D., Szmigiel, D., and Zielinski, J., *Catal. Lett.* **68**, 163 (2001).
9. Bielawa, H., Hinrichsen, O., Birkner, A., and Muhler, M., *Angew. Chem. Int. Ed.* **40**, 1061 (2001).
10. Happel, J., *Chem. Eng. Sci.* **33**, 1567 (1978).
11. Nwalor, J. U., Goodwin, J. G., Jr., and Biloen, P., *J. Catal.* **117**, 121 (1989).
12. Nwalor, J. U., and Goodwin, J. G., Jr., *Top. Catal.* **1**, 285 (1994).
13. McClaine, B. C., and Davis, R. J., *J. Catal.* **210**, 387 (2002).
14. Shannon, S. L., and Goodwin, J. G., Jr., *Chem. Rev.* **95**, 677 (1995).
15. McClaine, B. C., Siporin, S. E., and Davis, R. J., *J. Phys. Chem. B* **105**, 7525 (2001).
16. Ali, S. H., and Goodwin, J. G., Jr., *J. Catal.* **176**, 3 (1998).
17. Ali, S. H., and Goodwin, J. G., Jr., *J. Catal.* **170**, 265 (1997).
18. Ali, S. H., and Goodwin, J. G., Jr., *J. Catal.* **171**, 339 (1997).
19. Forni, L., Molinari, D., Rossetti, I., and Pernicone, N., *Appl. Catal. A* **185**, 269 (1999).
20. Kowalczyk, Z., Jodzis, S., Rarog, W., Zielinski, J., and Pielaszek, J., *Appl. Catal. A* **173**, 153 (1998).
21. Kowalczyk, Z., Jodzis, S., Rarog, W., Zielinski, J., Pielaszek, J., and Presz, A., *Appl. Catal. A* **184**, 95 (1999).
22. Liang, C., Wei, Z., Xin, Q., and Li, C., *Appl. Catal. A* **208**, 193 (2001).
23. Rossetti, I., Pernicone, N., and Forni, L., *Appl. Catal. A* **208**, 271 (2001).
24. Zeng, H. S., Hihara, T., Inazu, K., and Aika, K. I., *Catal. Lett.* **76**, 193 (2001).

25. Aika, K., Hori, H., and Ozaki, A., *J. Catal.* **27**, 424 (1972).
26. Mortensen, J. J., Hammer, B., and Norskov, J. K., *Phys. Rev. Lett.* **80**, 4333 (1998).
27. Dahl, S., Sehested, J., Jacobsen, C. J. H., Tornqvist, E., and Chorkendorff, I., *J. Catal.* **192**, 391 (2000).
28. Dietrich, H., Jacobi, K., and Ertl, G., *Surf. Sci.* **377–379**, 308 (1997).
29. Benndorf, C., and Madey, T. E., *Chem. Phys. Lett.* **101**, 59 (1983).
30. Dahl, S., Logadottir, A., Egeberg, R. C., Larsen, J. H., Chorkendorff, I., Tornqvist, E., and Norskov, J. K., *Phys. Rev. Lett.* **83**, 1814 (1999).
31. Dahl, S., Tornqvist, E., and Chorkendorff, I., *J. Catal.* **192**, 381 (2000).
32. Jacobsen, C. J. H., Dahl, S., Hansen, P. L., Tornqvist, E., Jensen, L., Topsoe, H., Prip, D. V., Moenshaug, P. B., and Chorkendorff, I., *J. Mol. Catal. A* **163**, 19 (2000).
33. Datye, A. K., Logan, A. D., and Long, N. J., *J. Catal.* **109**, 76 (1988).
34. Cisneros, M. D., and Lunsford, J. H., *J. Catal.* **141**, 191 (1993).
35. Gustafson, B., and Lunsford, J., *J. Catal.* **74**, 393 (1982).
36. Hansen, T., Wagner, J. B., Hansen, P. L., Dahl, S., Topsoe, H., and Jacobsen, C. J. H., *Science* **294**, 1508 (2001).